

1

2

Journal of Geophysical Research: Atmospheres

3

Supporting Information for

4

Improvement and Uncertainties of Global Simulation of Sulfate Concentration and Radiative Forcing in CESM2

5

6

Wendong Ge¹, Junfeng Liu¹, Songlin Xiang¹, Yuhan Zhou¹, Jingcheng Zhou¹, Xiurong Hu², Jianmin Ma¹, Xuejun Wang¹, Yi Wan¹, Jianying Hu¹, Zhaobin Zhang¹, Xilong Wang¹, Shu Tao¹

7

8

¹Laboratory for Earth Surface Processes, College of Urban and Environmental Sciences, Peking University, Beijing, 100871, China

9

10

² College of Economics and Management, Nanjing University of Aeronautics and Astronautics, Nanjing, 211106, China

11

12

13

Contents of this file

14

15

Figures S1 to S5

16

Table S1

17

18

Introduction

19

20

Figure S1 is monthly averaged surface sulfate concentrations in 2015. Figure S2 is vertical profiles of sulfate concentrations over different regions. Figure S3 is the differences in annual averaged sulfate radiative forcing between different cases in 2015. Figures S4 and S5 are the differences in annual global-mean sulfate radiative forcing distribution between the sensitivity tests and the Improved case in 2015. Table S1 is the description of all model simulations.

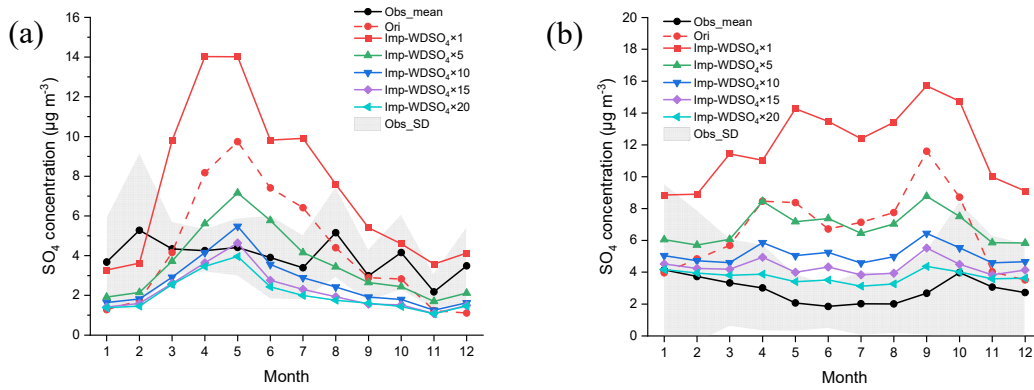
21

22

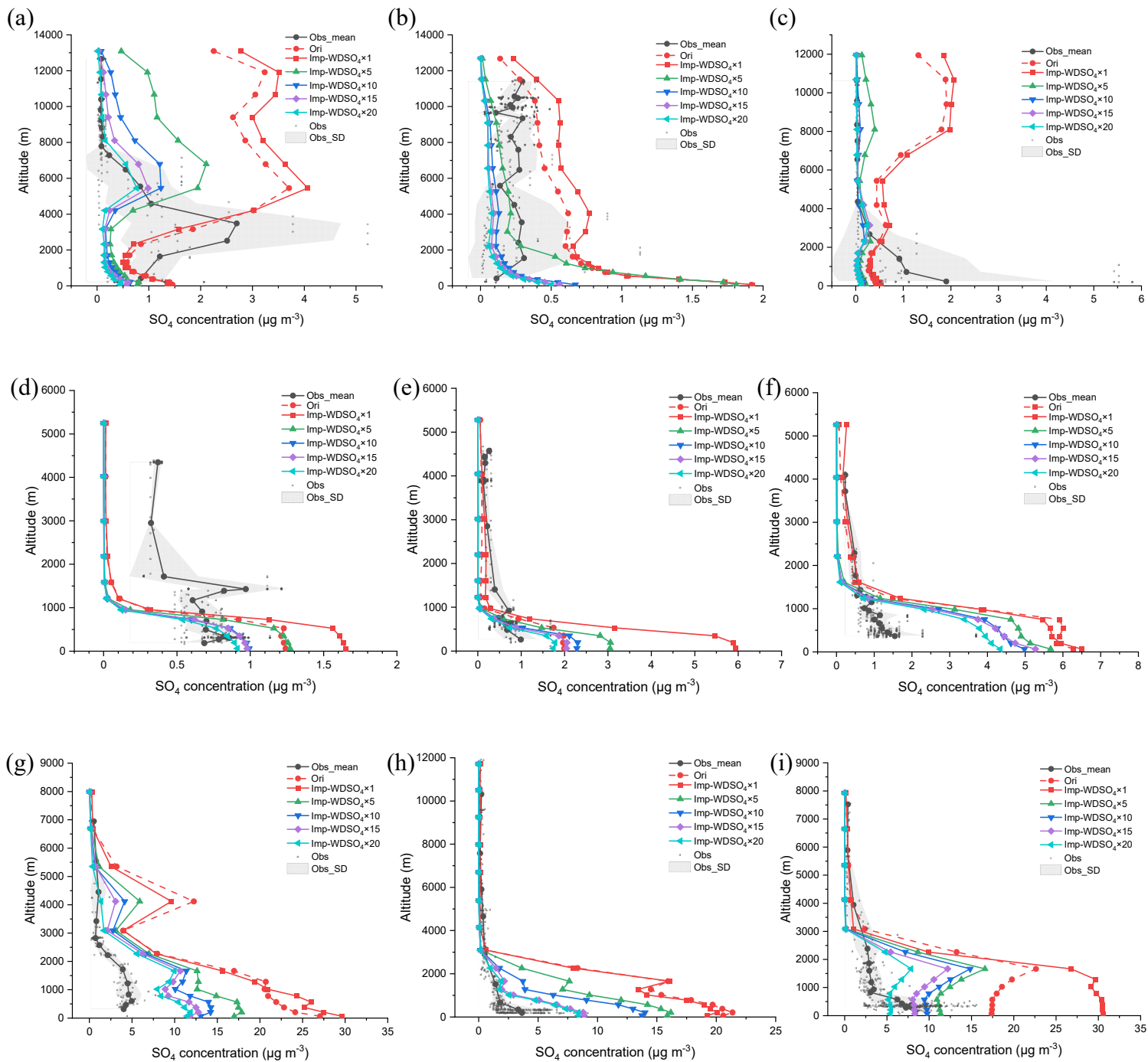
23

24

25



26 **Figure S1.** Monthly averaged surface sulfate concentrations ($\mu\text{g}\cdot\text{m}^{-3}$) in (a) Japan and South
 27 Korea and (b) other Asia countries in 2015. The black solid lines and red dashed lines represent the
 28 observed and Original simulated concentrations, respectively. Other lines represent
 29 improved sulfate concentrations with different levels of sulfate wet deposition fluxes. The
 30 multiples of sulfate wet deposition from top to bottom are 1, 5, 10, 15 and 20 (i.e., the
 31 Improved case). The gray areas represent the standard deviation of the observed
 32 concentrations. The corresponding monitoring network is EANET.
 33

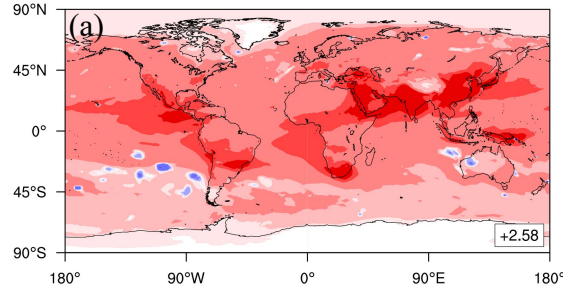


34

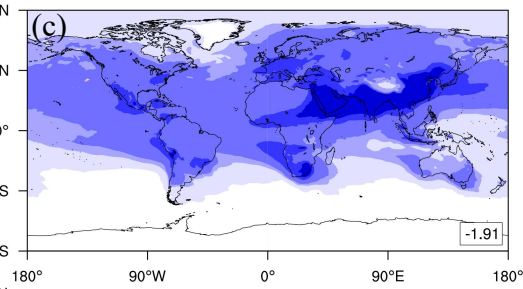
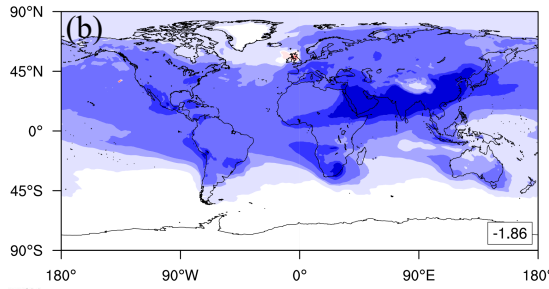
35 **Figure S2.** Vertical profiles of sulfate concentrations ($\mu\text{g}\cdot\text{m}^{-3}$) over different regions. The black solid lines represent
 36 the averaged observed concentrations at different altitudes. The red dashed lines represent the Original simulated
 37 concentrations in the same day of 2015. Other lines represent improved sulfate concentrations with different levels
 38 of sulfate wet deposition fluxes. The multiples of sulfate wet deposition from top to bottom are 1, 5, 10, 15 and 20
 39 (i.e., the Improved case). The gray areas represent the standard deviation of observed concentrations. The black
 40 dots represent every single observational data. The corresponding aircraft measurement campaigns are (a-c) ATom
 41 on 29 July 2016, 1 August 2016 and 6 August 2016, (d-f) WINTER on 1 March 2015, 7 March 2015 and 12 March 2015
 42 and (g-i) KORUS-AQ on 1 May 2016, 21 May 2016 and 4 June 2016.

43

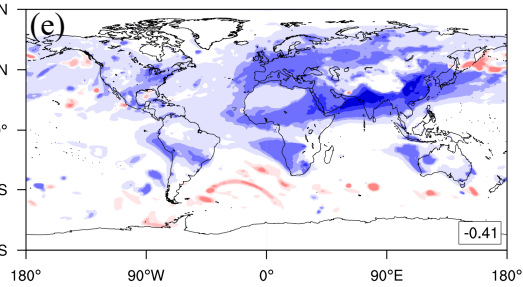
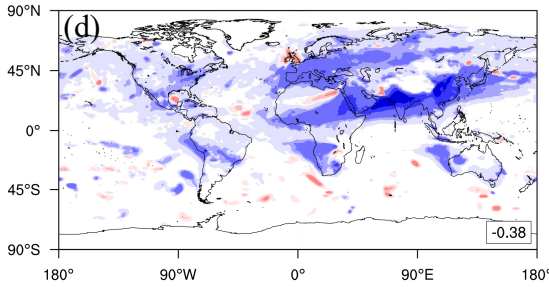
44



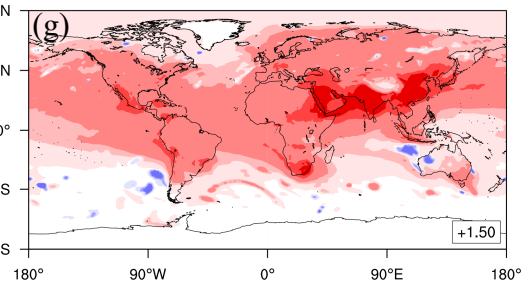
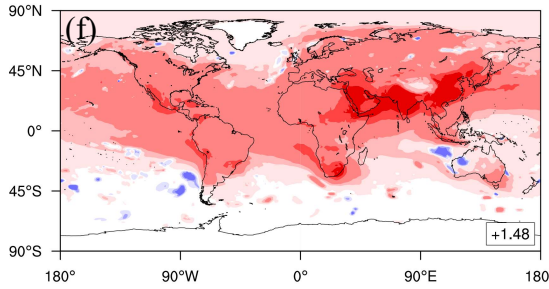
45



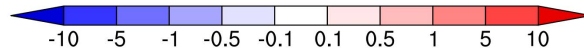
46



47



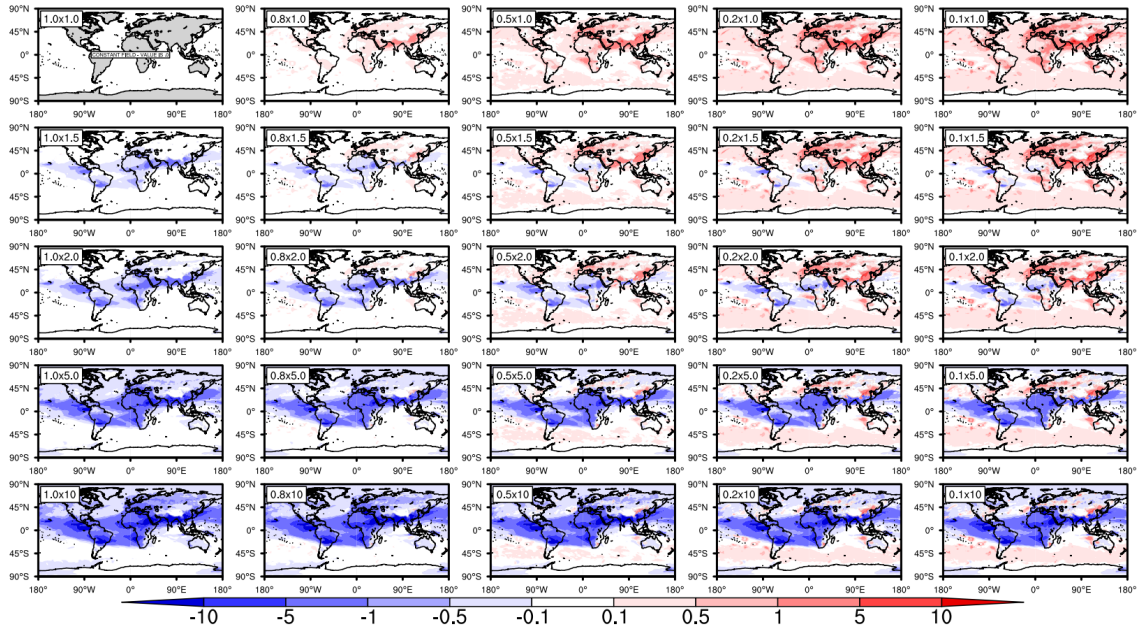
48



49

Figure S3. (a) The differences in annual averaged sulfate radiative forcing (unit: $W \cdot m^{-2}$) between the Improved case and the Original case in 2015 after the incorporation of detailed in-cloud aqueous-phase chemical mechanisms and multiplication of the wet deposition flux of sulfate. (b) and (d) are the radiative forcing of Original simulated and Improved simulated sulfate from 1850 to 2015. (c) and (e) are the radiative forcing of Original simulated and Improved simulated sulfate from all anthropogenic emissions in 2015. (f) The differences in sulfate radiative forcing between (b) and (d). (g) The differences in sulfate radiative forcing between (c) and (e). The values in the corner are annual global-mean radiative forcing (unit: $W \cdot m^{-2}$).

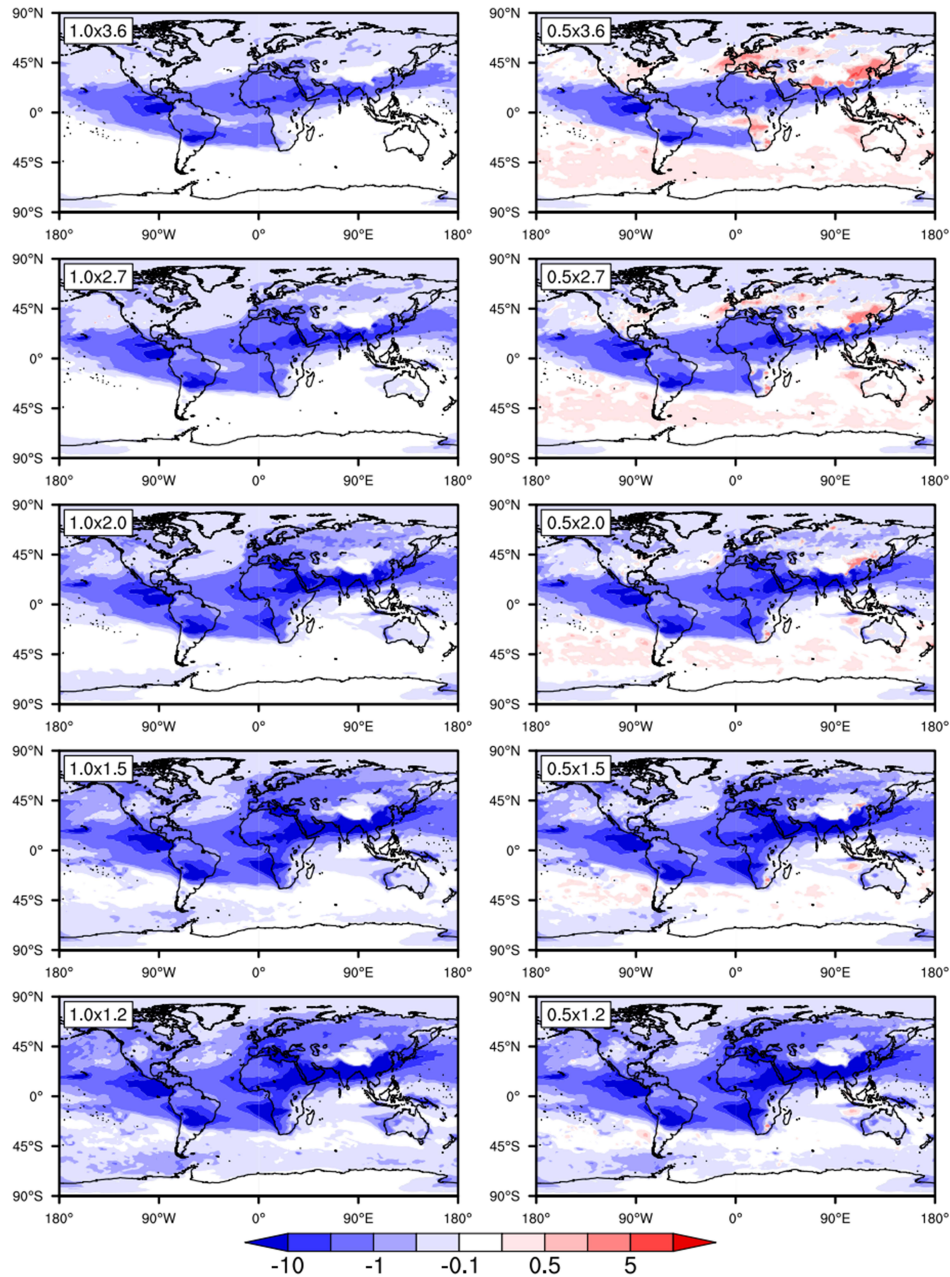
58



59

60 **Figure S4.** The differences in annual global-mean sulfate radiative forcing distribution (unit:
 61 $W \cdot m^{-2}$) between the sensitivity tests and the Improved case in 2015. The horizontal direction is
 62 the sensitivity test for decreasing the sulfate concentration at low altitudes (below 2.0 km).
 63 The decrease factors from left to right are 1.0, 0.8, 0.5, 0.2, and 0.1, indicating that the sulfate
 64 concentrations below 2.0 km are 100%, 80%, 50%, 20% and 10% of the Improved case,
 65 respectively. The vertical direction is the sensitivity test for increasing the sulfate
 66 concentration at high altitudes (above 2.0 km). The increase factors from top to bottom are
 67 1.0, 1.5, 2.0, 5.0, and 10.

68



69

70 **Figure S5.** The differences in annual global-mean sulfate radiative forcing distribution (unit:
 71 $W \cdot m^{-2}$) between the sensitivity tests and the Improved case in 2015. The vertical direction is
 72 the sensitivity test for changing the altitude of the turning point (TP, the altitude above which
 73 the model tends to underestimate sulfate concentrations and below which the model tends to
 74 overestimate sulfate concentrations). The altitudes of the TP are set from bottom to top as 1.2,
 75 1.5, 2.0, 2.7, and 3.6 km. The decreasing factors for sulfate concentration at low altitudes are
 76 1.0 and 0.5, and the increasing factor for sulfate concentration at high altitudes is 10.

77

Table S1. Description of all model simulations.

No.	Case name	Location in the paper	Description
1	CESM-Ori	Sections 3.1, 3.2, 3.3	The present-day Original case without any modification to the model.
2~6	CESM-Imp-WDSO ₄	Sections 3.1, 3.2, 3.3	The wet deposition of sulfate $\times 1, 5, 10, 15$ and 20 (i.e., the present-day Improved case) with the incorporation of detailed in-cloud aqueous-phase chemical mechanisms, respectively.
7	CESM-Ori-1850		The preindustrial (1849-1850) Original case (only replaced the SO ₂ emissions).
8	CESM-Imp-1850		The preindustrial Improved case.
9	CESM-Ori-anthro		The present-day Original case without any anthropogenic sources of sulfate.
10	CESM-Imp-anthro		The present-day Improved case without any anthropogenic sources of sulfate.
11	PORT-Ori	Sections 4.1, 4.2	The calculation of radiative forcing for case 1.
12	PORT-Imp	Sections 4.1, 4.2, 5	The calculation of radiative forcing for case 6.
13	PORT-Ori-1850	Section 4.2	The calculation of radiative forcing for case 7.
14	PORT-Imp-1850	Section 4.2	The calculation of radiative forcing for case 8.
15	PORT-Ori-anthro	Section 4.2	The calculation of radiative forcing for case 9.
16	PORT-Imp-anthro	Section 4.2	The calculation of radiative forcing for case 10.
17~20	PORT-high	Section 5	The calculation of radiative forcing when increasing the sulfate concentration ($\times 1.5, 2.0, 5.0$ and 10) at high altitudes.
21~24	PORT-low	Section 5	The calculation of radiative forcing when decreasing the sulfate concentration ($\times 0.8, 0.5, 0.2$ and 0.1) at low altitudes.
25~40	PORT-high \times low	Section 5	The calculation of radiative forcing when increasing the sulfate concentration at high altitudes and decreasing the concentration at low altitudes simultaneously, including $1.5\times 0.8, 1.5\times 0.5, 1.5\times 0.2, 1.5\times 0.1, 2.0\times 0.8, 2.0\times 0.5, 2.0\times 0.2, 2.0\times 0.1, 5.0\times 0.8, 5.0\times 0.5, 5.0\times 0.2, 5.0\times 0.1, 10\times 0.8, 10\times 0.5, 10\times 0.2$ and 10×0.1 .
41~48	PORT-height	Section 5	The calculation of radiative forcing when changing the turning point.